INTERNATIONAL JOURNAL OF INTEGRATED ENGINEERING
ISSN: 2229-838X e-ISSN: 2600-7916

IJIE

Vol. 17 No. 9 (2025) 149-160
https://publisher.uthm.edu.my/ojs/index.php/ijie

Synthesis and Characterization of Electrode with Pd-Ni/C Catalyst and Performance Test of MEA for Applications in Proton Exchange Membrane Fuel Cell (PEMFC)

Dwi Hawa Yulianti[1,2,4], Dedi Rohendi[1,3,4]*, Edy Herianto Majlan[5], Addy Rachmat[1,3,4], Dilla Nursyahfitri[4], Nyimas Febrika Sya'baniah[1,2,4], Icha Amelia[4]

[1] *Faculty of Mathematics and Natural Sciences, Universitas Sriwijaya, Jalan Srijaya Negara, Bukit Lama, Kec. Ilir Barat I, Palembang, 30139, INDONESIA*
[2] *Chemistry program, Faculty of Computer and Science, Universitas Indo Global Mandiri, Jl. Jendral Sudirman No.629 Km.4, Palembang, 30129, INDONESIA*
[3] *Departement of Chemistry, Faculty of Mathematic and Natural Sciences, Universitas Sriwijaya, Jl. Palembang-Prabumulih Km 32 Indralaya, Ogan Ilir, 30662, INDONESIA*
[4] *Center of Research Excellent in Fuel Cell and Hydrogen, Universitas Sriwijaya, Jl. Srijaya Negara Bukit Lama Palembang, 30138, INDONESIA*
[5] *Fuel Cell Institute, Universiti Kebangsaan Malaysia, Bangi 43600, Selangor DE, MALAYSIA*

*Corresponding Author: rohendi19@unsri.ac.id
DOI: https://doi.org/10.30880/ijie.2025.17.09.010

Article Info

Received: 2 October 2025
Accepted: 22 July 2025
Available online: 31 December 2025

Keywords

Pd-Ni/C, ratio, impregnation, MEA, PEMFC

Abstract

The implementation of Pd-Ni/C catalysts in PEMFCs is still quite limited, even though Pd and Ni alloys hold considerable promise as an alternative to decrease reliance on Pt/C. The Pd-Ni/C metal alloy functions as a catalyst on the anode side for the hydrogen oxidation process in PEMFCs. The catalyst was synthesized by incorporating $NiCl_2 \cdot 6H_2O$ into Pd/C with a catalyst loading of 0.5 mg/cm^2. Electrodes were prepared with varying Pd to Ni weight ratios in carbon (3:1, 1:1, and 1:3), and were compared against Pd/C and Ni/C electrodes, while a Pt/C catalyst was used on the cathode side. The Membrane Electrode Assembly (MEA) was constructed by combining the anode containing the Pd-Ni/C catalyst, and the cathode containing the Pt/C catalyst using a Nafion 212 membrane. XRD characterization showed a carbon peak at 2θ = 26.4° and a palladium peak at 2θ = 41°, both with low intensity. XRD spectrum of Pd-Ni/C electrode showing amorphous crystal peaks. The highest catalytic activity of the electrode was achieved by the electrode with Pd:Ni = 3:1 with an ECSA value of 1.539 m^2/g and conductivity value of 3.98 × 10^{-2} S/cm. The highest OCV value was obtained with the MEA using a Pd/C catalyst at ambient temperature, reaching 0.88 V, which was not significantly different from the 0.8 V value of the Pd:Ni= 3:1 catalyst. The maximum power density of MEA with Pd:Ni= 3:1 catalyst at the anode was 4.67 mW/cm^2 at a current density of 14.4 mA/cm^2. This research indicates that the MEA with the Pd:Ni = 3:1 catalyst at anode achieves optimal performance at an operating temperature of 25°C, contributing to high efficiency in PEMFC applications.

1. Introduction

Proton Exchange Membrane Fuel Cell (PEMFC) is one type of fuel cell that is very promising to be developed as an energy producer in the future. In addition, PEMFC can operate well at low temperatures with high efficiency, is environmentally friendly, and is free of noise pollution [1–3]. PEMFC has attracted a lot of attention with the use of fuel in the form of hydrogen so that it can produce electricity with high energy density [4]. Another advantage of using hydrogen as a fuel is that it can be an alternative to minimizing the use of fossil fuels by converting chemical energy into electrical energy [5].

In PEMFCs, hydrogen gas is oxidized at the anode to produce protons and electrons, which then interact with oxygen gas supplied from the cathode [6]. Meanwhile, a semipermeable membrane made of the solid electrolyte Nafion 212 enables the transport of protons (hydrogen ions) from the anode to the cathode [7]. The most commonly used catalyst in PEMFCs is platinum supported on carbon (Pt/C), due to its high catalytic activity for both Oxygen Reduction Reaction (ORR) and hydrogen oxidation reactions (HOR) [8]. However, the high cost and limited availability of Pt have prompted research into finding more economical yet effective alternative catalysts. One approach that has been studied to a limited extent involves the use of metal alloys, such as palladium (Pd) and nickel (Ni), which present attractive alternatives [9]. Palladium has catalytic properties similar to those of platinum, including an excellent ability to break H-H bonds in hydrogen molecules [10]. Additionally, Pd is cheaper and more abundant compared to Pt, making it a promising choice for alternative catalysts [11]. Conversely, nickel is known for its low cost and abundant availability. Ni also possesses good catalytic capabilities for certain redox reactions and can enhance the stability and durability of the catalyst when alloyed with other metals [12].

The addition of nickel to a Pd alloy improves thermal and mechanical stability and enhances electrical conductivity, crucial for efficient electron flow during electrochemical reactions [13]. Better conductivity is crucial for facilitating efficient electron flow during electrochemical reactions in PEMFCs, thereby improving the overall efficiency of the fuel cell. A Pd-Ni alloy offers several significant advantages as a catalyst in PEMFCs. Combining these metals can generate a synergistic effect that enhances overall catalytic activity. Pd provides high catalytic activity, while Ni offers stability and cost-effectiveness. Moreover, Pd-Ni alloy demonstrates higher tolerance to poisons like carbon monoxide (CO), which can contaminate the catalyst on the anode side of PEMFC, an essential factor for long-term operation [14].

Although a Pd-Ni alloy shows great potential as a catalyst, several challenges need to be addressed. Optimization of the alloy composition is necessary to maximize catalytic efficiency. Additionally, developing efficient and scalable production methods poses a challenge for commercial applications [15]. Further studies are required to understand the degradation mechanisms of the Pd-Ni alloy and how to enhance its durability under real operating conditions. With continuous research, a Pd-Ni alloy has the potential to become a competitive alternative to platinum-based catalysts, aiding the adoption of cleaner and more sustainable energy technologies. This development can bring us closer to the widespread implementation of PEMFCs as a reliable and economical source of clean energy in the future. In this paper, we developed an MEA with a cathode containing a Pt catalyst and an anode containing a Pd-Ni/C catalyst, as well as Nafion-212 as the electrolyte membrane, where Pd-based catalyst exhibit higher current density than Pt-based catalyst making them a promising alternative for fuel cell anodes [14].

2. Methodology

2.1 Synthesis of Pd-Ni/C Catalyst

The synthesis of the Pd-Ni/C catalyst was conducted using the impregnation method of $NiCl_2 \cdot 6H_2O$ onto a 40 wt% Pd/C catalyst, with a catalyst loading of 0.5 mg/cm^2 and an electrode size of 5 × 5 cm^2. $NiCl_2 \cdot 6H_2O$ catalyst was dissolved in deionized water, then impregnated into Pd/C and stirred for 24 hours with the addition of NH_4OH for each Pd ratio of 3:1, 1:1, and 1:3. The mixture was subsequently filtered, and the precipitate was washed with deionized water and dried in an oven at 110 °C for 3 hours. This was followed by calcination in a furnace at 550 °C for 5 hours and reduction using H_2 gas at a flow rate of 1 mL/s at 400 °C for 2 hours, resulting in the Pd-Ni/C catalyst product. The synthesis process of the Pd-Ni/C catalyst is depicted in Fig. 1. A similar procedure is used for the formation of Ni/C catalyst. This catalyst is made by mixing 40 wt% $NiCl_2 \cdot 6H_2O$ into carbon, while the Pt/C catalyst uses a commercial catalyst.

Int. Journal of Integrated Engineering Vol. 17 No. 9 (2025) p. 149-160

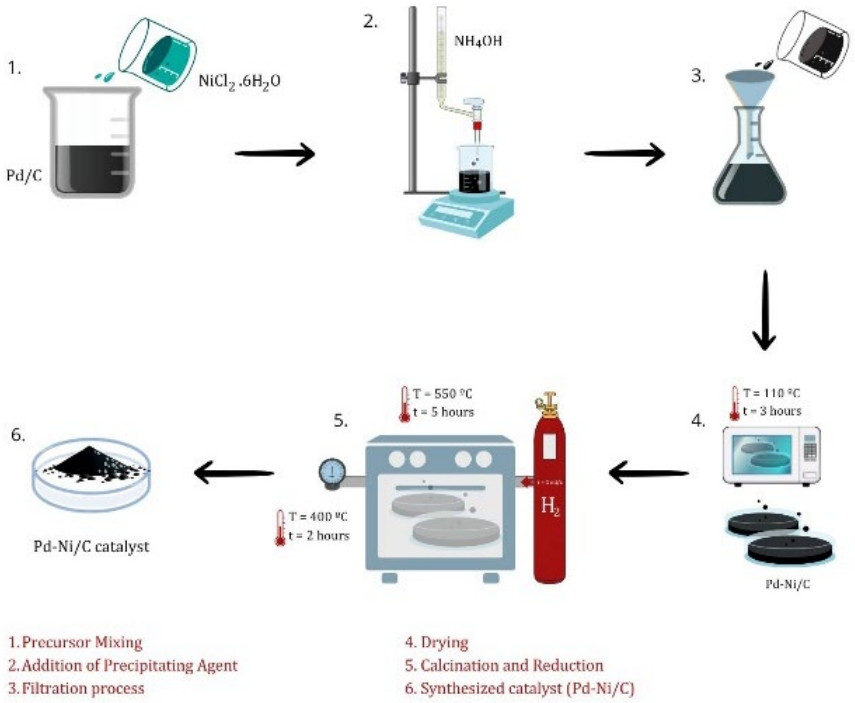

Fig. 1 *Synthesis of Pd-Ni/C catalyst by impregnation method*

2.2 Fabrication of Electrode

The fabricated electrode consists of a cathode with a Pt/C catalyst containing 12 wt% Pt/C and an anode with Pd/C, Pd-Ni/C, and Ni/C catalysts, each with a loading of 0.5 mg/cm^2. The Pd and Ni weight ratio on the anode varies as follows: 3:1, 1:1, and 1:3. The catalyst was dissolved in 2-propanol, and Nafion solution was added, then stirred for 30 minutes using an ultrasonic homogenizer. PTFE was added, and the mixture was stirred again for 30 minutes to form an ink. The Pd-Ni/C ink was sprayed onto a 25 cm^2 Gas Diffusion Layer (GDL) alternately in horizontal and vertical directions until fully deposited, then sintered in a furnace at 350°C for 3 hours, maximizing the backing layer's hydrophobicity [16]. The same process was applied to electrodes with Pt/C, Pd/C, and Ni/C catalysts.

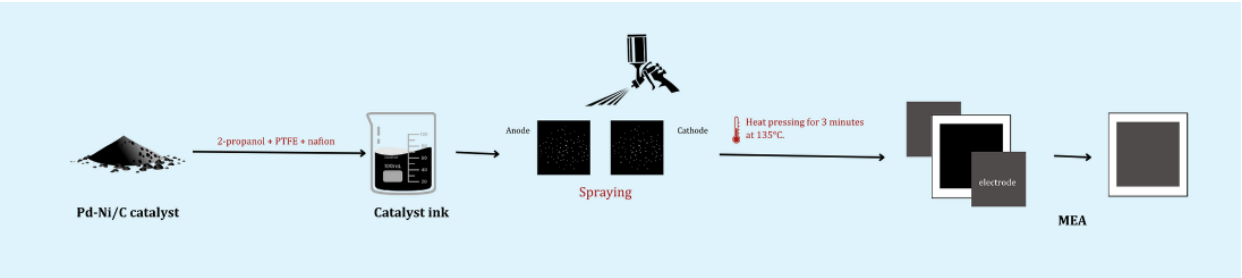

Fig. 2 *Electrode fabrication process using the spraying method.*

2.3 Characterization and Electrochemical Evaluation of Electrode

The crystal structure of the Pd-Ni/C catalyst, distributed on the electrodes, was examined using X-ray Diffraction (XRD). The electrochemical properties of the catalyst were further analyzed using a Methrohm PGSTAT204 Autolab potentiostat/galvanostat, employing an Ag/AgCl reference electrode, platinum as a counter electrode, and the Pd-Ni/C catalyst as the working electrode in a 1 M NaOH solution [17]. Electrochemical Surface Area (ECSA) values were measured using Nova 2.1.4 software with the Cyclic Voltammetry method, in a potential range of -0.4 V to 0.8 V at a scanning speed of 0.025 V/s. The ECSA value can be calculated based on the average charge for hydrogen via the Eq. (1) [18].

$$ECSA\ \frac{m^2}{g} = \frac{Q_H\ [\mu C] x\ 10}{405\ [\mu C\ .cm^{-2}]\ x\ Pd_{loading}\ [mg]} \quad (1)$$

where *QH* represents the average charge for hydrogen adsorption, obtained by integrating the area under the hydrogen adsorption peak, while 405 μC.cm^{-2} cm^2 is the transfer coefficient of the Pd crystalline active surface area. Additionally, Electrochemical Impedance Spectroscopy (EIS) was performed to assess the conductivity of the electrocatalyst, using the FRA Impedance method on Nova 2.1.4 software to observe the impedance response to an applied voltage of 1.2 V. Eq. (2) was used to determine the electrical conductivity σ [S/cm], where L [cm] represents the thickness of the electrode, A [cm^2] represents its surface area, and R [Ohm] represents the observed resistance [19].

$$\sigma = L/R \times A \tag{2}$$

2.4 MEA Performance Test

The MEA with an active area of 25 cm^2 was tested in a single-cell configuration using the WonAtech SMART2 Fuel Cell Test Station, resulting in polarization curves based on the I-V and I-P performance curves. The MEA was installed in a stack consisting of two bipolar plates with a pin-type design. The installation was adjusted to a high level of tightness to ensure no gas leakage (0.5 – 1.5 N m) [20]. The experiment was conducted under operating conditions the temperature of the humidifier is 65°C, gas flow rates of 200 mL/min and a relative humidity of 85-87% [3].

3. Results and Discussion

3.1 X-Ray Diffraction (XRD) Analysis

Characterizing the crystallinity and structure of electrochemical catalysts is crucial for understanding their physical and chemical properties and their impact on performance. X-ray Diffraction (XRD) is a widely used technique for identifying crystal phases and determining particle sizes on electrode surfaces [21]. The Pd-Ni/C catalyst, which combines palladium (Pd) and nickel (Ni) on a carbon base, is popular in fuel cells and other electrochemical applications due to its excellent catalytic properties. Analyzing its distribution and crystal structure provides insights into how these elements enhance electrochemical reaction efficiency. However, its use in PEMFCs is still limited compared to Pt-based catalysts.

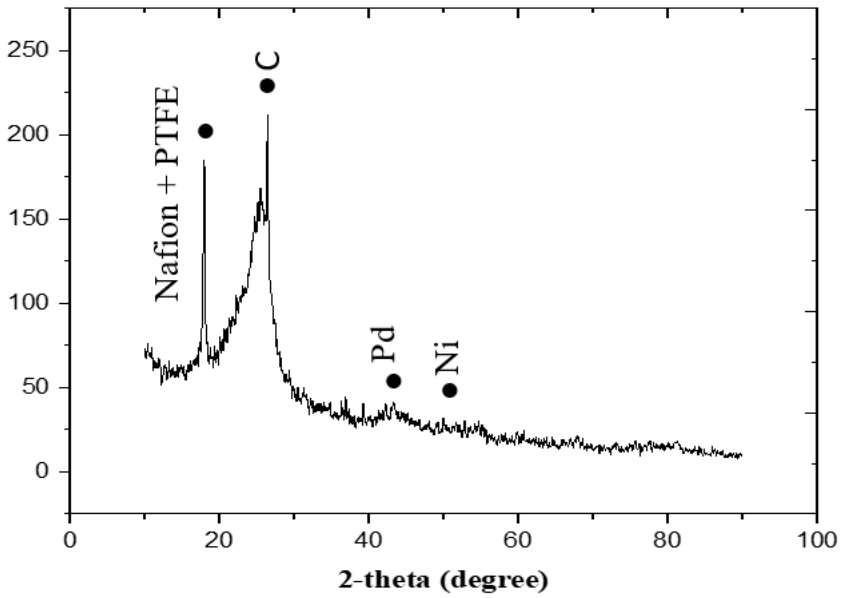

Fig. 3 *Electrode diffractogram with Pd-Ni/C catalyst (Pd:Ni = 1:1)*

The XRD analysis for the electrode with Pd-Ni/C catalyst is presented in Fig. 3. The diffractogram shows a carbon peak at 2θ = 26.4° and a palladium peak around 2θ = 41°, suggesting an amorphous structure for the Pd-Ni alloy [22]. The diffraction pattern of Pd/C typically appears at 2θ = 40°, but the addition of nickel shifts the alloy formation angle. Additionally, the amorphous polymer structure of Nafion peaks at 17°, while crystalline PTFE peaks between 17.9° and 18.6°. The overlapping diffraction peaks of Nafion and PTFE between 12° and 20° contribute to close diffraction angles [23]. This analysis provides valuable insights into the interactions within the Pd-Ni/C catalyst and the effect of each component's crystal structure on overall performance. The electrode

Int. Journal of Integrated Engineering Vol. 17 No. 9 (2025) p. 149-160

diffractogram analysis, corroborated by JCPDS data (04-0850 and 46-1043), shows that nickel typically appears at 2θ = 45.45° and 51.8°, and palladium at 2θ = 40.1° and 46.6°, with (111) and (200) face-centered cubic (fcc) crystal lattices (JCPDS card no. 05-0681) [24-25].

3.2 Electrochemical Characterization

3.2.1 Cyclic Voltammetry (CV)

The electrodes with Pd-Ni/C catalyst were characterized using the CV method to analyze the electrochemical properties based on the ECSA values indicating the Pd-Ni/C electrocatalytic activity. CV measurements were carried out using a 1 M NaOH as an electrolyte solution, the reference electrode was an Ag/AgCl electrode, where if there was a current flowing on the electrode, the Cl^- concentration would change and the potential would change. The auxiliary electrode used is Pt metal which functions to maintain a constant value of the comparison electrode potential because the counter electrode has a small resistance from the Ag/AgCl electrode [17,26]. The results of CV measurements on electrodes with varying Pd-Ni and Pt/C ratios can be seen in Fig. 4.

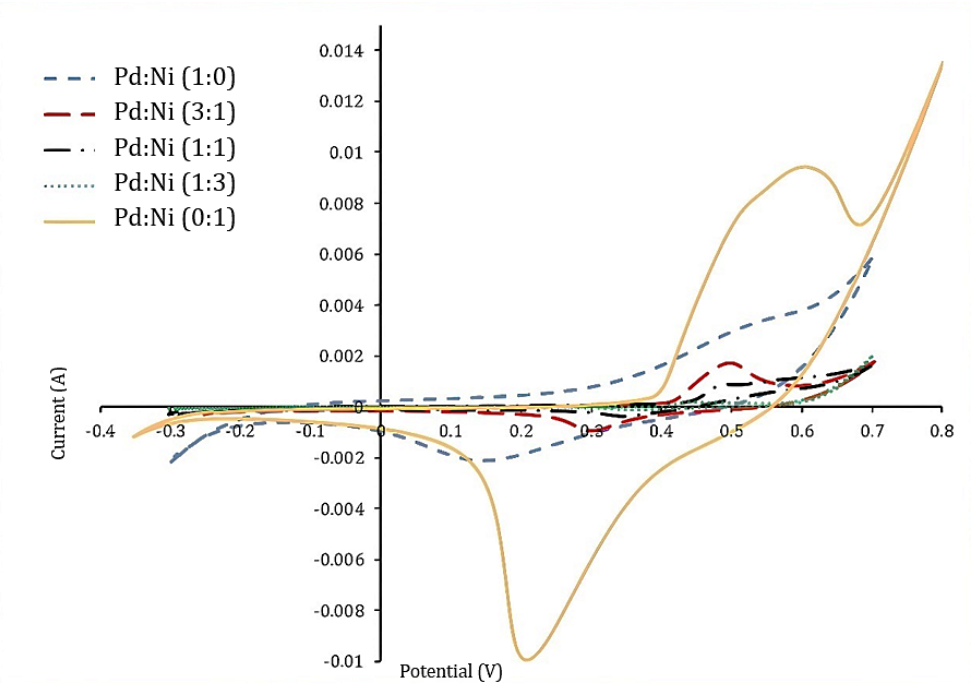

Fig. 4 *Voltammogram of electrodes*

Fig. 4 presents voltammograms for hydrogen adsorption and desorption on electrodes with various Pd and Ni ratios, where the active surface area is determined by the potential applied to the working electrode. To evaluate the reversibility of the anodic and cathodic peaks, cyclic voltammograms were recorded over different potential ranges in both positive and negative directions [20-21]. The variation in Pd and Ni weight ratios influences electrocatalytic performance, particularly in terms of conductivity, stability, and active surface area. Nickel (Ni) has higher conductivity than palladium (Pd), resulting in a broader voltammogram curve due to a wider charge distribution and greater double-layer capacitance. However, Pd is more stable in electrochemical environments, especially under acidic conditions, as it is more resistant to corrosion compared to Ni, which is prone to oxidation. Therefore, while Ni enhances conductivity, Pd remains crucial for maintaining electrocatalytic stability and performance.

Compared to Pd/C and Ni/C, the combination of Pd-Ni/C can provide a synergistic effect; however, at certain ratios, the Electrochemically Active Surface Area (ECSA) tends to decrease. Individually, Pd/C and Ni/C exhibit higher ECSA, while mixed Pd-Ni/C shows a reduction due to surface structure modifications and possible alloy formation, which reduces the number of active sites. At specific ratios, such as Pd-Ni/C 1:3, the ECSA is the lowest, indicating that an excessive Ni content can negatively impact electrocatalytic activity. The presence of a peak in the desorption region indicates the release of previously adsorbed species, such as hydrogen or oxides, reflecting the catalyst's active surface area and stability. Changes in the desorption peak intensity can signify degradation or structural modifications of the catalyst after electrochemical cycling, which affects long-term electrocatalytic performance. The results of the CV analysis were used to estimate the active surface area using an electrochemical

approach based on the Electrochemical Surface Area (ECSA) values of Pt/C and Pd-Ni/C electrode as shown in Table 1.

Table 1 *Calculation of ESCA electrode value*

Electrode	Scan Rate (V/s)	Qh (μC)	ECSA (m^2/g)
Pd/C	0.025	5.07×10^{-3}	2.502
Pd-Ni/C (3:1)	0.025	3.12×10^{-3}	1.539
Pd-Ni/C (1:1)	0.025	1.92×10^{-3}	0.948
Pd-Ni/C (1:3)	0.025	0.58×10^{-3}	0.285
Ni/C	0.025	5.73×10^{-2}	2.231
Pt/C	0.025	0.1×10^{-2}	0.956

Table 1 presents the effect of mixing Pd and Ni at various weight ratios, including Pd-Ni/C (3:1), Pd-Ni/C (1:1), and Pd-Ni/C (1:3). In all these variations, nickel acts as a bridge between the catalyst nanoparticles and the support material, leading to lower electrochemical impedance and stronger alloy interactions. However, due to the difference in particle sizes between Pd and Ni, uniform size distribution was not achieved, resulting in a reduction in the active surface area. This effect is not limited to Pd-Ni/C (1:1) but is also observed in Pd-Ni/C (3:1) and Pd-Ni/C (1:3), where the addition of nickel influences the overall alloy size. The excessive presence of Ni in Pd-Ni/C (1:3) further contributes to a significant decrease in the Electrochemically Active Surface Area (ECSA), indicating that an imbalance in composition can negatively impact catalytic performance and electron transfer efficiency.

3.2.2 Electrochemical Impedence Spectroscopy (EIS)

The response of the electrode in a certain frequency range is in the form of a real impedance value (Z') or resistance and an imaginary impedance value (-Z") or capacitance. If the value of Z' is greater than Z" when the resistance is large, the current flowing at the electrode will be hampered. In addition, EIS can be used to measure the conductivity of electrodes in fuel cells. To describe the resistance in the circuit, an electronic circuit simulation was performed using Nyquist curve fitting. When plotted as Z' versus Z", it produces the Nyquist curve and equivalent circuit models shown in Fig. 5 and 6.

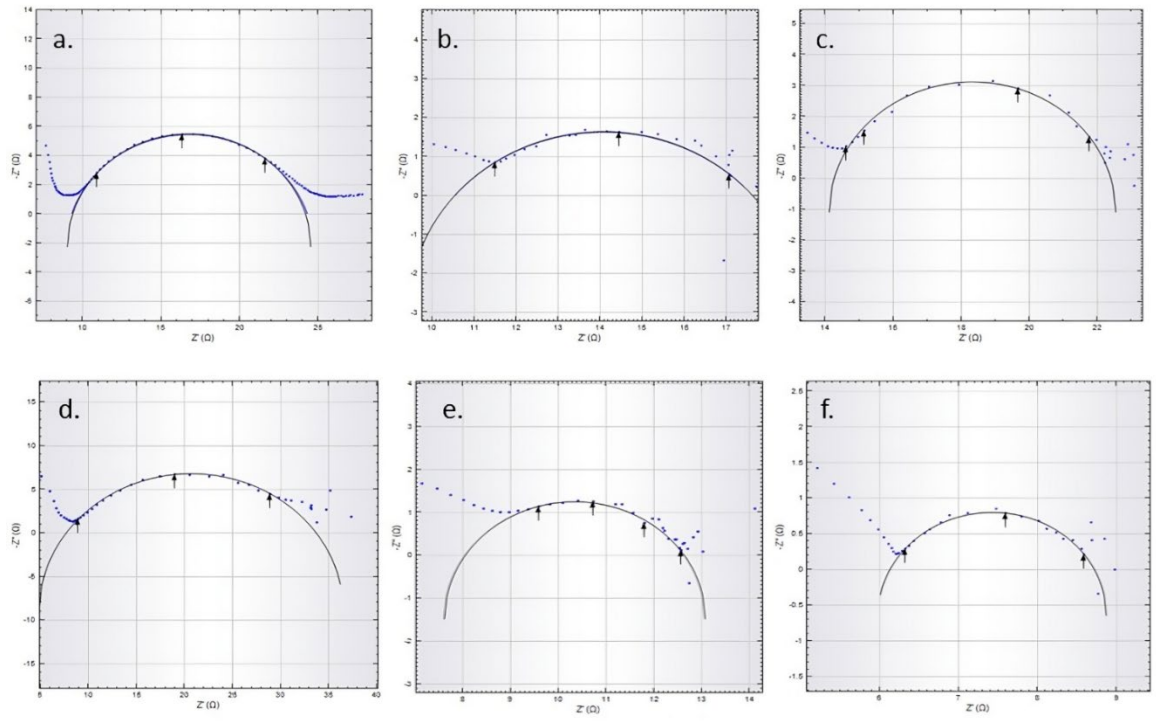

Fig. 5 *Nyquist plot of the electrodes with (a) Pd/C; (b) Pd-Ni/C (3:1); (c) Pd-Ni/C (1:1); (d) Pd-Ni/C(1:3); (e) Ni/C and (f) Pt/C catalyst*

Int. Journal of Integrated Engineering Vol. 17 No. 9 (2025) p. 149-160

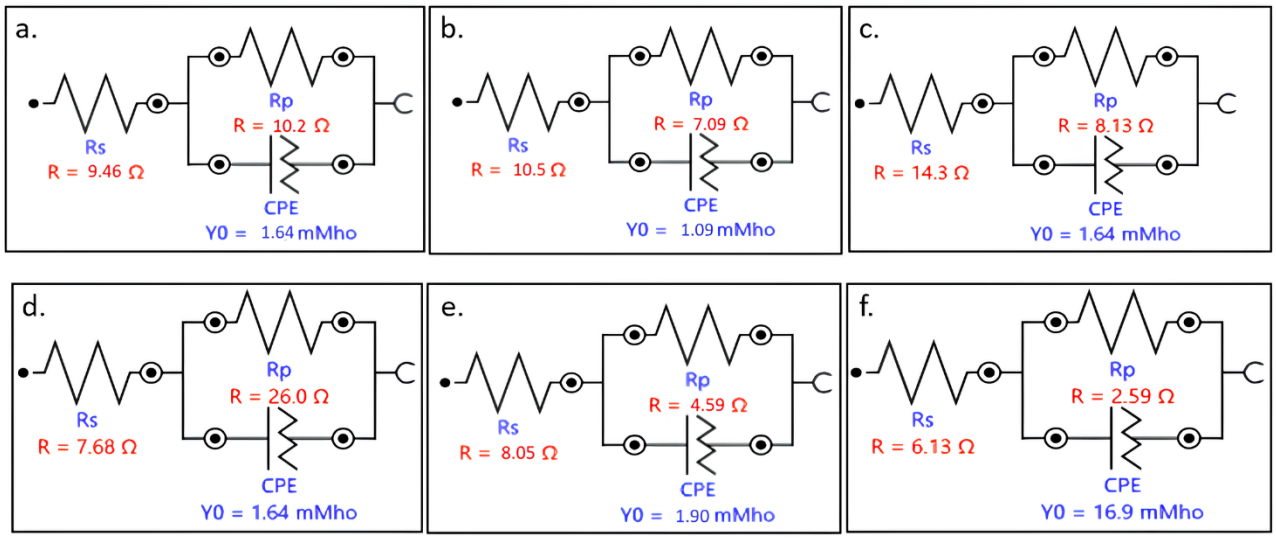

Fig. 6 *Equivalent circuit models for electrodes (a) Pd/C; (b) Pd-Ni/C (3:1); (c) Pd-Ni/C (1:1); (d) Pd-Ni/C(1:3); (e) Ni/C; and (f) Pt/C catalyst*

The resistance in the Nyquist plot is determined by fitting the data to an equivalent circuit model, considering charge transfer and ohmic resistance to ensure accurate impedance representation. Based on EIS analysis, the addition of Ni to Pd/C affects the impedance value. The greater the impedance, the more hindered the capacity or ability of electrons to flow through the electrode [27]. Low cell impedance occurs due to overload at high frequencies. As the voltage increases, electron transfer decreases, reflecting an increase in the strength of the electrochemical cell at the electrode surface. However, there are cases where the curved impedance curve will increase with rising overvoltage due to the influence of conductivity and mass transfer in the catalyst layer. The conductivity value was obtained by measuring the electrode coated with a Pd-Ni/C catalyst, which was then connected to the Metrohm PGSTAT204N Autolab Potentiostat using the EIS method. The fitting on the Nyquist plot simulates an electronic circuit, displaying data on the values of Rs (series resistance) and Rp (parallel resistance) on the monitor screen to determine the electrical conductivity of an electrode. The results of the electrical conductivity test can determine the ability of an electrode related to the overall performance and efficiency of the catalyst. The electrical conductivity value can be calculated using the formula in Eq. (1).

Table 2 *Electrode conductivity value*

Electrode	Impedance		Conductivity
	Rs (Ω)	Rp (Ω)	(S/cm)
Pd/C (1:0)	9.46	10.2	3.39×10^{-2}
Pd-Ni/C (3:1)	10.54	7.09	3.78×10^{-2}
Pd-Ni/C (1:1)	14.26	8.13	2.98×10^{-2}
Pd-Ni/C (1:3)	7.68	26.02	1.98×10^{-2}
Ni/C (0:1)	8.05	4.59	5.27×10^{-2}
Pt/C	6.13	2.58	7.65×10^{-2}

Table 2 shows the results of electrical conductivity calculations using Eq. (2), indicating an increase of approximately 11.5% after the addition of Ni to Pd-Ni/C (3:1) electrodes compared to Pd/C catalysts. However, a decrease in conductivity occurs at the same or higher Ni addition ratios compared to Pd in Pd-Ni/C catalysts. This is due to structural or phase changes resulting from the combination of two metals in a bimetallic configuration. Meanwhile, Ni/C and Pt/C electrodes exhibit high electrical conductivity because they consist of a single metal (monometallic) and are not affected by other metals. Other factors that also influence electrical conductivity include concentration, ion mobility, ion valence, and temperature.

3.3 MEA Performance Testing

The single stack MEA made by combining the electrodes with Pt/C catalyst at the cathode and the electrodes of Pd-Ni/C with varying composition at the anode was tested by measuring the open circuit voltage (OCV), I-V, and

I-P Performance on the PEMFC stack connected to the WonAtech Smart 2. The single-cell configuration is illustrated in Fig. 7 to enhance understanding of the experimental setup.

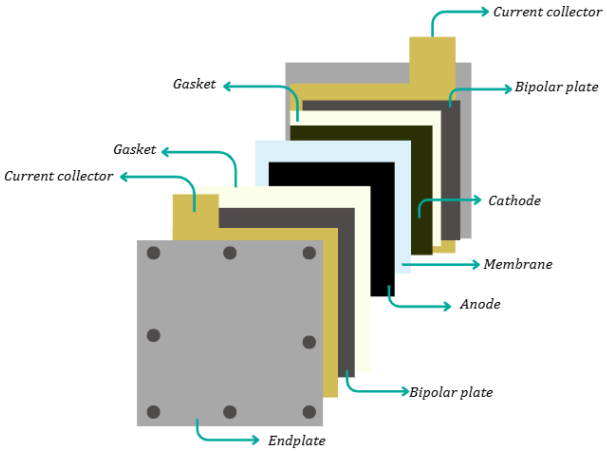

Fig. 7 *Schematic representation of a single cell PEMFC stack*

Before performance testing, the MEA was first activated for 1 hour to ensure stability. The fuel for PEMFC is in the form of hydrogen gas at the anode and oxygen gas at the cathode at stack temperature of 25°C with the humidifier temperature of 65 °C. OCV measurements in the MEA are carried out to determine the performance of the MEA before the load is added.

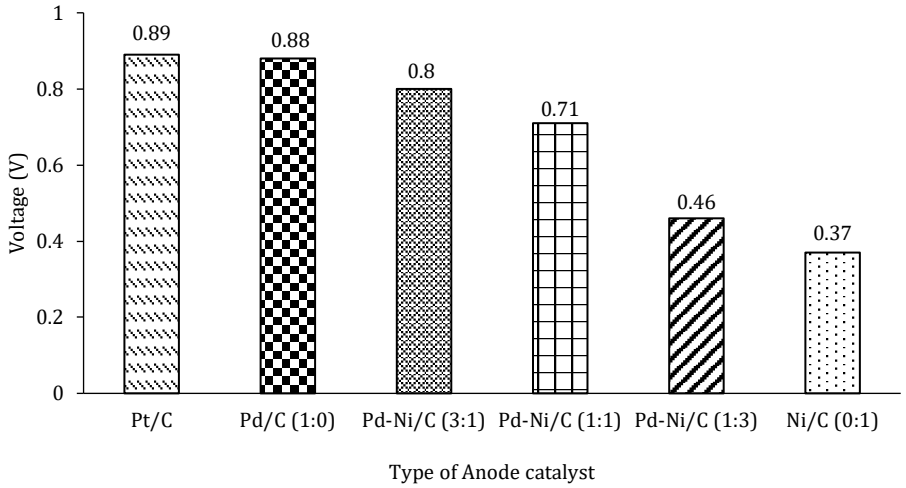

Fig. 8 *OCV value of MEA*

The measurement of the OCV reflects the initial electrode potential when interacting with the fuel source in a PEMFC [28]. In the MEA, the addition of Ni decreases the OCV value, as indicated in Fig. 8. However, the MEA with the Pd-Ni/C (3:1) catalyst exhibits an OCV of 0.80 V, which demonstrates a better initial condition compared to MEAs using the Pd-Ni/C (1:1) and Pd-Ni/C (1:3) catalysts. A similar trend is observed in Ni/C (0:1), which demonstrates high ECSA and electrical conductivity (Table 1 and 2) values but a low OCV. This may be due to interfacial resistance between Ni/C (0:1) and Pt/C. When the electrode is integrated into the MEA, interfacial resistance may increase due to imperfections in the contact between the catalyst layer and the electrolyte membrane, hindering the transfer of electrons and ions. This resistance can be further exacerbated by differences in the intrinsic properties of the materials, suboptimal pore distribution, and interactions between Ni and other components in the MEA structure. The overall performance of the MEA can be analyzed through the polarization curve shown in Fig. 9.

Int. Journal of Integrated Engineering Vol. 17 No. 9 (2025) p. 149-160

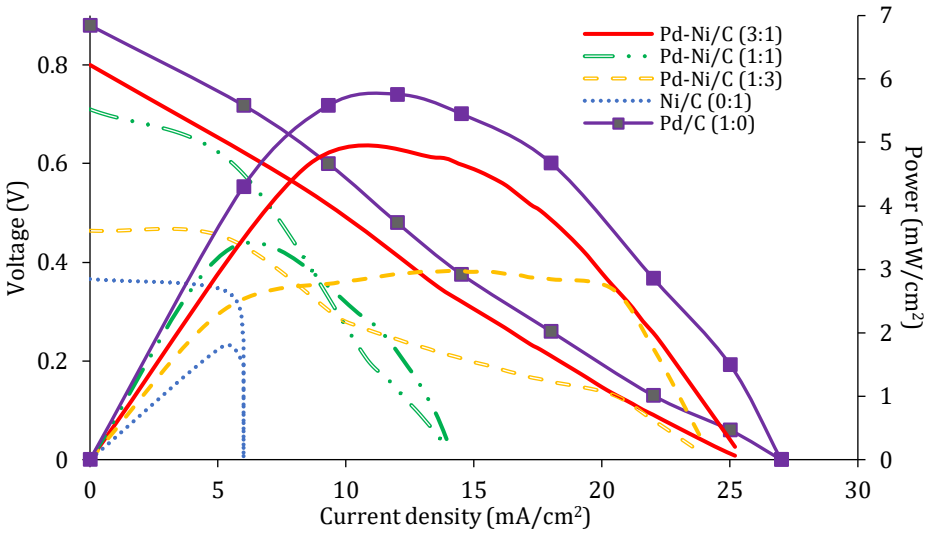

Fig. 9 *Polarization curve of the MEA with different anode catalyst variations*

Fig. 9 demonstrates the relationship between increasing current and its effects on both voltage and power for various MEAs, where performance metrics are directly proportional to the OCV of each MEA. The Pd/C MEA exhibits the most favorable performance characteristics among the tested compositions, due to its superior ability to sustain voltage despite rising current. In comparison, the MEA with Pd-Ni/C (3:1) catalyst shows enhanced performance over those with Pd-Ni/C (1:1), Pd-Ni/C (1:3), and Ni/C, attaining a maximum power density of 4.67 mW/cm^2 at a current density of 14.4 mA/cm^2. This indicates that a higher power density indicates better performance efficiency in the MEA.

The operational conditions of the MEA with Pd-Ni/C (3:1) catalyst were also analyzed based on performance degradation influenced by stack temperature. Stack temperature affects the humidity within the proton exchange membrane fuel cell (PEMFC) and can enhance reaction kinetics. However, excessive stack temperatures can cause cracking and damage to the MEA due to excessive drying or inadequate hydration. The performance degradation of the MEA with Pd-Ni/C (3:1) catalyst is shown in Fig. 10.

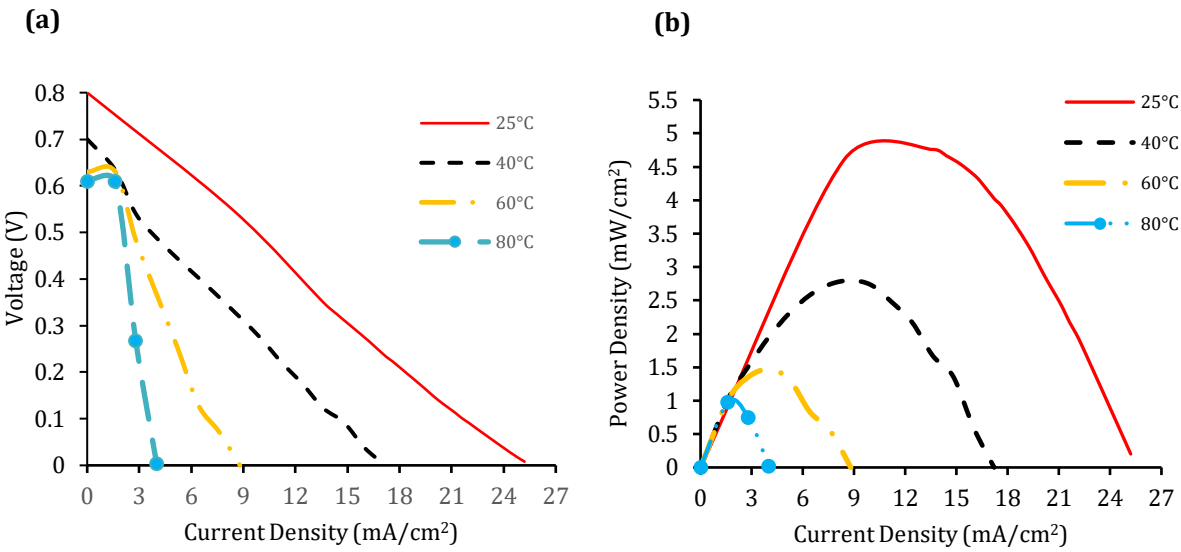

Fig. 10 *MEA performance degradation influenced by stack temperature (a) I-V (b) I-P curve*

Fig. 10 shows the MEA performance at a stack temperature of 25°C. Performance degradation of the MEA increases with a rising stack temperature, thus it is recommended to operate at room temperature (25°C).

Operating under these conditions provides benefits in energy efficiency. Additionally, optimal temperature management can extend the lifespan of the MEA components and reduce maintenance needs, thereby lowering the overall operational costs of the system. The decrease in performance of the Pd-Ni/C (3:1) catalyst at high temperatures can be caused by particle melting or aggregation, material degradation, material migration from the surface, undesirable side reactions, and carbonization that reduces catalytic activity. Another cause is the degradation of carbon materials, which accelerate with operational temperature. Additionally, both electrochemical and chemical corrosion are accelerated by the presence of platinum at the cathode. Platinum not only increases the rate of electrochemical reactions but also contributes to the susceptibility of corrosion. In other words, the degradation of carbon materials and the acceleration of corrosion caused by platinum lead to reduced durability and performance of components in the system [29].

4. Conclusion

The use of Pd-Ni/C catalysts in PEMFCs shows promise as an alternative to reduce dependence on Pt/C catalysts. These catalysts are effective for hydrogen oxidation on the anode side. They were synthesized by mixing $NiCl_2 \cdot 6H_2O$ into Pd/C with a catalyst loading of 0.5 mg/cm^2. Electrodes were prepared with various Pd-Ni ratios in carbon (Pd-Ni/C (3:1), Pd-Ni/C (1:1), and Pd-Ni/C (1:3)) and compared with Pd/C and Ni/C electrodes, with Pt/C used on the cathode side. The resulting MEA combined these electrodes with a Nafion 212 membrane. XRD characterization revealed carbon peaks at $2\theta = 26.4°$ and palladium peaks at $2\theta = 41°$, both with low intensity. The Pd-Ni/C electrodes showed no significant nickel peaks in their XRD spectra. The highest catalytic activity was achieved by Pd-Ni/C (3:1) with an ECSA value of 1.539 m^2/g and conductivity of 3.98×10^{-3} S/cm. In performance tests, the MEA using Pd/C and Pd-Ni/C (3:1) catalysts exhibited nearly comparable OCV values of 0.88 V and 0.8 V, respectively, with a maximum power density of 4.67 mW/cm^2 at a current density of 14.4 mA/cm^2. These findings underscore the potential of Pd-Ni/C catalysts, especially at a Pd-Ni/C (3:1), to improve PEMFC performance as an alternative to platinum-based catalysts. This research indicates that the Pd-Ni/C (3:1) catalyst achieves optimal performance at an operating temperature of 25°C, contributing to high efficiency in PEMFC applications.

Acknowledgement

The authors express their gratitude to the Center of Research Excellent in Fuel Cell and Hydrogen at Universitas Sriwijaya for providing laboratory analysis and support and to Universitas Indo Global Mandiri for their invaluable assistance.

Conflict of Interest

The authors declare that there is no conflict of interest regarding the publication of the paper.

Author Contribution

The authors confirm their contribution to the paper as follows: ***study conception and design:*** *Dedi Rohendi, Edy Herianto Majlan, Dwi Hawa Yulianti;* ***data collection:*** *Dilla Nur Syafitri and Addy Rachmat;* ***analysis and interpretation of results:****, Nyimas Febrika, and Icha Amelia;* ***draft manuscript preparation:*** *Dwi Hawa Yulianti, Dedi Rohendi. All authors reviewed the results and approved the final version of the manuscript.*

References

[1] Pourrahmani, H., Yavarinasab, A., Siavashi, M., & Matian, M. (2022). Progress in the proton exchange membrane fuel cells (PEMFCs) water/thermal management: From theory to the current challenges and real-time fault diagnosis methods. *Energy Reviews*, *1*(1), 100002. https://doi.org/10.1016/j.enrev.2022.100002

[2] Ermis, K., Toklu, E., & Yegin, M. (2020). Investigation of operating temperature effects on PEM fuel cell. *Journal of Engineering Research and Applied Science*, *9*(2), 1538-1545.

[3] Rohendi, D., Syarif, N., Arsali, Yulianti, D. H., Anjeli, N. R., Febrika S., N., Amelia, I. (2023, December 26) Effect of Humidifier Temperature and Hydrogen Flow Rate on MEA Performance of PEMFC Using Pt/C and Pd-Co/C Catalyst. *Malaysian Journal of Chemistry, 25*(5), 223-229, https://doi.org/10.55373/mjchem.v25i5.223

[4] Hooshyari, K., Amini Horri, B., Abdoli, H., Fallah Vostakola, M., Kakavand, P., & Salarizadeh, P. (2021). A review of recent developments and advanced applications of high-temperature polymer electrolyte membranes for PEM fuel cells. *Energies*, *14*(17), 5440, https://doi.org/10.3390/en14175440

[5] Tashie-Lewis, B. C., & Nnabuife, S. G. (2021). Hydrogen production, distribution, storage and power conversion in a hydrogen economy-a technology review. *Chemical Engineering Journal Advances*, *8*, 100172, https://doi.org/10.1016/j.ceja.2021.100172

[6] Rustana, C. E., Muchtar, S. J., Sugihartono, I., Sasmitaningsihhiadayah, W., Madjid, A. D. R., & Hananto, F. S. (2021, October). The effect of voltage and electrode types on hydrogen production from the seawater electrolysis process. In *Journal of Physics: Conference Series* (Vol. 2019, No. 1, p. 012096). IOP Publishing. https://doi.org/10.1088/1742-6596/2019/1/012096

[7] Zhu, L. Y., Li, Y. C., Liu, J., He, J., Wang, L. Y., & Lei, J. D. (2022). Recent developments in high-performance Nafion membranes for hydrogen fuel cells applications. *Petroleum Science*, *19*(3), 1371-1381, https://doi.org/10.1016/j.petsci.2021.11.004

[8] Etesami, M., Mehdipour-Ataei, S., Somwangthanaroj, A., & Kheawhom, S. (2022). Recent progress of electrocatalysts for hydrogen proton exchange membrane fuel cells. *International Journal of Hydrogen Energy*, *47*(100), 41956-41973, https://doi.org/10.1016/j.ijhydene.2021.09.133

[9] Montserrat-Siso, G., & Wickman, B. (2022). PdNi thin films for hydrogen oxidation reaction and oxygen reduction reaction in alkaline media. *Electrochimica Acta*, *420*, 140425, https://doi.org/10.1016/j.electacta.2022.140425

[10] Czarnomysy, R., Radomska, D., Szewczyk, O. K., Roszczenko, P., & Bielawski, K. (2021). Platinum and palladium complexes as promising sources for antitumor treatments. *International journal of molecular sciences*, *22*(15), 8271, https://doi.org/10.3390/ijms22158271

[11] Ramli, Z. A. C., Pasupuleti, J., Saharuddin, T. S. T., Yusoff, Y. N., Isahak, W. N. R. W., Baharudin, L., Chong, T. Y., Koh, S. P., & Kiong, S. T. (2023). Electrocatalytic activities of platinum and palladium catalysts for enhancement of direct formic acid fuel cells: An updated progress. *Alexandria Engineering Journal*, *76*, 701-733, https://doi.org/10.1016/j.aej.2023.06.069

[12] Franceschini, F., & Taurino, I. (2022). Nickel-based catalysts for non-enzymatic electrochemical sensing of glucose: A review. *Physics in Medicine*, *14*, 100054, https://doi.org/10.1016/j.phmed.2022.100054

[13] Chen, X., Li, J., Wang, Y., Zhou, Y., Zhu, Q., & Lu, H. (2020). Preparation of nickel-foam-supported Pd/NiO monolithic catalyst and construction of novel electric heating reactor for catalytic combustion of VOCs. *Applied Catalysis A: General*, *607*, 117839, https://doi.org/10.1016/j.apcata.2020.117839

[14] Huang, Y., Wu, P., Ma, Y., Tang, J., Zhou, X., Ma, X., ... & Lin, D. (2023). Single atom iron carbons supported Pd–Ni–P nanoalloy as a multifunctional electrocatalyst for alcohol oxidation. *International Journal of Hydrogen Energy*, *48*(37), 13972-13986, https://doi.org/10.1016/j.ijhydene.2022.12.274

[15] Şahin, Ö., Akdag, A., Horoz, S., & Ekinci, A. (2023). Synthesized PdNi/C and PdNiZr/C catalysts for single cell PEM fuel cell cathode catalysts application. *Fuel*, *346*, 128391, https://doi.org/10.1016/j.fuel.2023.128391

[16] D. Rohendi, E. H. Majlan, A. B. Mohamad, W. R. W. Daud, A. A. H. Kadhum, and L. K. Shyuan, "Effect of PTFE content and sintering temperature on the properties of a fuel cell electrode backing layer," *J. Fuel Cell Sci. Technol.*, vol. 11, no. 4, pp. 1–6, 2014, https://doi.org/10.1115/1.4026932

[17] Alotaibi, N., Hammud, H. H., Al Otaibi, N., & Prakasam, T. (2020). Electrocatalytic properties of 3D hierarchical graphitic carbon–cobalt nanoparticles for urea oxidation. *ACS omega*, *5*(40), 26038-26048. https://doi.org/10.1021/acsomega.0c03477

[18] Eshghi, A., Behbahani, E. S., Kheirmand, M., & Ghaedi, M. (2019). Pd, Pd–Ni and Pd–Ni–Fe nanoparticles anchored on MnO2/Vulcan as efficient ethanol electro-oxidation anode catalysts. *International Journal of Hydrogen Energy*, *44*(52), 28194-28205, https://doi.org/10.1016/j.ijhydene.2019.08.236

[19] Biancolli, A. L. G., Konovalova, A., Santiago, E. I., & Holdcroft, S. (2023). Measuring the ionic conductivity of solid polymer electrolyte powders. *International Journal of Electrochemical Science*, *18*(10), 100288, https://doi.org/10.1016/J.IJOES.2023.100288

[20] Ul Hassan, N., Kilic, M., Okumus, E., Tunaboylu, B., & Murat Soydan, A. (2016). Experimental determination of optimal clamping torque for AB-PEM fuel cell. *Journal of Electrochemical Science and Engineering*, *6*(1), 9-16, https://doi.org/10.5599/jese.198

[21] Ali, A., Chiang, Y. W., & Santos, R. M. (2022). X-ray diffraction techniques for mineral characterization: A review for engineers of the fundamentals, applications, and research directions. *Minerals*, *12*(2), 205, https://doi.org/10.3390/min12020205

[22] Saha, S., Gayen, P., Wang, Z., Dixit, R. J., Sharma, K., Basu, S., & Ramani, V. K. (2021). Development of bimetallic PdNi electrocatalysts toward mitigation of catalyst poisoning in direct borohydride fuel cells. *ACS Catalysis*, *11*(14), 8417-8430, https://doi.org/10.1021/acscatal.1c00768

[23] Li, X., Qian, L., Liu, L., Liu, Z., Zhang, H., Yang, L., Zhang, D., Chen, Z., Fang, P., & He, C. (2023). Extra highways for proton diffusion in TiO2@ MIL-101-Cr/Nafion composite membranes with high single-cell performance. *Journal of Power Sources*, *564*, 232906, https://doi.org/10.1016/j.jpowsour.2023.232906

[24] Jiang, D., Shi, Y., Zhou, L., Ma, J., Yin, C., Lin, Q., & Pan, H. (2024). Exploring the key role of electronic effects in Pd catalysts supported on Ni-modified N-doped porous carbon for direct synthesis of H2O2 under atmospheric pressure. *Molecular Catalysis*, *565*, 114407, https://doi.org/10.1016/j.mcat.2024.114407

[25] Smiljanic, M., Bele, M., Moriau, L., Ruiz-Zepeda, F., Šala, M., & Hodnik, N. (2021). Electrochemical stability and degradation of commercial Pd/C catalyst in acidic media. *The Journal of Physical Chemistry C*, *125*(50), 27534-27542, https://doi.org/10.1021/acs.jpcc.1c08496

[26] Kambale, S. V, Jadhav, A. L., Kore, R.M., & Thakur, A.V. (2019). Cyclic Voltammetric Study of CuO Thin Film Film Electrodes Prepared by Automatic Cyclic Voltammetric Study of CuO Thin Film Electrodes Prepared by Automatic Spray Pyrolysis. *Macromolecular Simposia*, 387, 1-3, https://doi.org/10.1002/masy.201800213

[27] Rohendi, D., Syarif, N., Rachmat, A., Mersitarini, D., Ardiyanta, D., Erliana, W. H., Mahendra, I., Febrika S., N., Yulianti, D. H., Amelia, I., & Reo, M. A. R. (2022). Effect of Milling Time and PCA on Electrode Properties of Cu2O-ZnO/C Catalyst Alloy used on Electrochemical Reduction Method of CO2. *International Journal of Integrated Engineering*, *14*(2), 186-192, https://doi.org/10.30880/ijie.2022.14.02.022

[28] Majlan, E. H., Rohendi, D., Daud, W. R. W., Husaini, T., & Haque, M. A. (2018). Electrode for proton exchange membrane fuel cells: A review. *Renewable and Sustainable Energy Reviews*, *89*, 117-134, https://doi.org/10.1016/j.rser.2018.03.007

[29] Pawlyta, M., Smykała, S., Liszka, B., Blacha-Grzechnik, A., Krzywiecki, M., Jurkiewicz, K., & Jakóbik-Kolon, A. (2023). Influence of carbon support structure on cathode catalysts durability. *Applied Surface Science*, *611*, 155637, https://doi.org/10.1016/j.apsusc.2022.155637